
Article:
Etxabide, A., Ribeiro, R.D.C., Guerrero, P. et al. (5 more authors) (2018) Lactose-crosslinked fish gelatin-based porous scaffolds embedded with tetrahydrocurcumin for cartilage regeneration. International Journal of Biological Macromolecules, 117. pp. 199-208. ISSN 0141-8130

https://doi.org/10.1016/j.ijbiomac.2018.05.154

Lactose-crosslinked fish gelatin-based porous scaffolds embedded with tetrahydrocurcumin for cartilage regeneration

A. Etxabide[a], R.D.C. Ribeiro[b], P. Guerrero[a], A.M. Ferreira[b], G.P. Stafford[c], K. Dalgarno[b], K. de la Caba[a], P. Gentile[b]*

[a] BIOMAT Research Group, University of the Basque Country (UPV/EHU), Escuela de Ingeniería de Gipuzkoa, Plaza de Europa 1, 20018 Donostia-San Sebastián, Spain.

[b] School of Engineering, Newcastle University, Claremont Road, Newcastle Upon Tyne, NE1 7RU, United Kingdom.

[c] School of Clinical Dentistry, University of Sheffield, 19 Claremont Crescent, Sheffield S10 2TA, United Kingdom.

*Corresponding author email: piergiorgio.gentile@ncl.ac.uk

Telephone number: +44 0191 208 3620

ABSTRACT

Tetrahydrocurcumin (THC) is one of the major colourless metabolites of curcumin and shows even greater pharmacological and physiological benefits. The aim of this work was the manufacturing of porous scaffolds as a carrier of THC under physiological conditions. Fish-derived gelatin scaffolds were prepared by freeze-drying by two solutions concentrations (2.5% and 4% w/v), cross-linked via addition of lactose and heat-treated at 105 °C. This cross-linking reaction resulted in more water resistant scaffolds with a water uptake capacity higher than 800%. Along with the cross-linking reaction, the gelatin concentration affected the scaffold morphology, as observed by scanning electron microscopy images, by obtaining a reduced porosity but larger pores sizes when the initial gelatin concentration was increased. These morphological

changes led to a scaffold's strength enhancement from 0.92±0.22MPa to 2.04±0.18MPa when gelatin concentration was increased. THC release slowed down when gelatin concentration increased from 2.5 to 4%w/v, showing a controlled profile within 96 h. Preliminary *in vitro* test with chondrocytes on scaffolds with 4%w/v gelatin offered higher metabolic activities and cell survival up to 14 days of incubation. Finally the addition of THC did not influence significantly the cytocompatibility and potential antibacterial properties were demonstrated successfully against *Staphylococcus aureus*.

KEYWORDS: Tetrahydrocurcumin; gelatin; lactose; scaffolds; antibacterial.

1. Introduction

Porous scaffolds are crucial for many biomedical and biological applications [1, 2]. In tissue engineering, compared with synthetic materials, natural polymers have been shown to favourably regulate division, adhesion, differentiation and migration of cells [3]. Gelatin was chosen as a base material because it is biocompatible, biodegradable, non-carcinogenic, less antigenic than collagen, and commercially available at relatively low cost [4, 5]. Moreover, it is recognised as safe material by the Food and Drug Administration. Therefore, porous gelatin scaffolds have found many applications in tissue engineering research, e.g. for bone, skin, cartilage and nerve regeneration [6-10]. In particular, tissue engineering of articular cartilage *in vitro* is a promising strategy for cartilage repair, in order to tackle the difficulties related with the self-repair of articular cartilage due to its avascular tissue nature, low rate of chondrocyte proliferation and matrix turnover [11]. Porous scaffolds are used to support cell adhesion and proliferation and to guide formation of cartilage tissue. However, *in vitro* engineered

46 cartilage often has thickness limitation, heterogeneous cartilage extracellular matrix
47 (ECM) and weak mechanical property which limit their clinical application [12, 13].
48 In order to preserve structure and provide mechanical support to cells during tissue
49 formation [14], a cross-linking of gelatin is required. Chemical cross-linking methods
50 typically use chemicals such as aldehydes, aspartic and glutamic acids [15].
51 Additionally, physical cross-linking methods, such as heating, drying, and irradiation, are
52 also commonly applied to proteins [16, 17]. In particular, in this work we considered the
53 effect of heating in the presence of sugars on modifying the conformation and
54 interactions within proteins, leading to a complex cross-linking process known as
55 Maillard reaction or non-enzymatic glycation. The main variables affecting the extension
56 of the Maillard reaction are temperature, time, initial pH, carbonyl/sugar ratio, and water
57 activity [18-20]. So, these factors should be analysed in order to obtain the properties
58 required for biomedical applications.
59 Additionally, gelatin-based scaffolds can be used as a vehicle for the release of
60 bioactive agents such as antioxidants, peptides, growth factors, antimicrobials and
61 drugs [21-24]. In particular, infection is a major problem in orthopaedics leading to
62 implant failure. Sources of infectious bacteria include the environment of the operating
63 room, surgical equipment, clothing worn by medical and paramedical staff, resident
64 bacteria on the patient's skin and bacteria already residing in the patient’s body [25].
65 Implant-associated infections are the result of bacteria adhesion to an implant surface
66 and subsequent biofilm formation at the implantation site [26]. In this work, we decided
67 to evaluate the antibacterial properties of the crosslinked gelatin scaffolds with the
68 incorporation of tetrahydrocurcumin (THC), a water-soluble, colourless and tasteless

69 antioxidant, antidiabetic, anticancer and anti-inflammatory plant-derived compound, that
70 is increasingly being used for pharmaceutical, medical and food applications [27, 28].
71 Literature reports only studies on the delivery of the hydrophobic compound curcumin to
72 facilitate wound healing with the addition of ethanol in chitosan-alginate sponges [29] or
73 cyclodextrins in slightly hydrated alginate foams in order to improve the distribution of
74 curcumin [30].

75 Therefore, beyond the state of the art, this is the first work where gelatin-based
76 scaffolds, prepared by freeze-drying, were cross-linked by using lactose. Lactose is a
77 disaccharide occurring almost exclusively in the milk of mammals with important
78 nutritional and probiotic properties and is mainly used in various food, nutrition and
79 pharmaceutical formulations [31]. In this study, lactose was used as a cross-linker in
80 order to promote the Maillard reaction, between the carbonyl group of lactose and the
81 gelatin amino group, and to improve the mechanical stability of the gelatin scaffolds.
82 Furthermore, THC was added to the initial gelatin solution to analyse the release of the
83 bioactive compound from the gelatin scaffold and its antibacterial effect in the presence
84 of the common nosocomial and joint-replacement/ wound infecting organisms
85 *Pseudomonas aeuroginosa* and *Staphylococcus aureus*.

86 This work aimed at studying the effect of initial gelatin concentration, cross-linking
87 reaction and THC addition on the physico-chemical, mechanical and biological
88 characteristics of porous gelatin scaffolds as potential medical device in
89 musculoskeletal tissue regeneration.

90 **2. Materials and methods**

91 *2.1 Materials*

92 A commercial cod fish gelatin type A was employed in this study. It has bloom 200,
93 11.06% moisture and 0.147% ash. Fish gelatin was kindly supplied by Weishardt
94 International (Liptovsky Mikulas, Slovakia) and meets the quality standard for edible
95 gelatin (1999/724/CE). Glycerol and lactose (Panreac, Barcelona, Spain) were used as
96 plasticizer and cross-linking agent, respectively. Tetrahydrocurcumin was gifted by
97 Sabinsa Corporation (East Windsor, New Jersey, USA) and was used as bioactive
98 agent.

99 *2.2 Scaffold preparation*

100 2.5 and 4% w/v fish gelatin porous scaffolds were prepared by freeze-drying. Firstly,
101 2.5 g or 4 g gelatin and 20 wt% lactose (on gelatin dry basis) were dissolved in 100 mL
102 distilled water for 30 min at 80 °C under continuous stirring to obtain a homogenous
103 blend. After that, a mixture of 10 wt% glycerol and 5 wt% THC (on gelatin dry basis)
104 was added to the solution, pH was adjusted to 10 with 1 N NaOH and the solution was
105 placed in an ultrasonic device (USC300TH, VWR International, USA) at room
106 temperature for 5 min. Subsequently, the solution was maintained at 80 ºC for 30 min
107 under stirring, 2 mL solution was poured into each well of a 24 multiwell plate (Costar
108 3526, Corning Incorporated, USA) and the plate was kept in the fridge at 4 ºC to cool
109 down. Once the solution was gelled, the plate was kept in a freezer at -20 ºC for 48 h
110 and then, freeze-dried for 48 h (Alpha 1-2 LDplus, CHRIST, Germany). Finally, non-
111 heated (NH) scaffolds were taken out from the wells and 1 day later some of them were
112 heat-treated (HT) at 105 ºC for 24 h in an oven (Carbolite 3000, Carbolite Gero, UK) in

113 order to promote the Maillard cross-linking reaction [32-34]. As verified in a previous
114 work [27], these conditions do not affect the thermal stability of gelatin and THC. The
115 samples containing THC and heat-treated were coded as HT-THC.

116 *2.3 Attenuated total reflection-Fourier transform infrared (ATR-FTIR) spectroscopy*

117 FTIR spectra were obtained using a Spectrum Two PE instrument equipped with a
118 horizontal attenuated total reflectance (ATR) crystal (ZnSe) (PerkinElmer Inc., USA).
119 The samples were placed directly onto the ATR crystal and spectra were collected in
120 transmittance mode. Each spectrum was the result of the average of 32 scans at 4 cm^{-1}
121 resolution. Measurements were recorded in the wavelength range of 1800-800 cm^{-1}. All
122 spectra were smoothed using the Savitzky-Golay function. Second-derivative spectra of
123 the amide region were used at bands position guides for the curve fitting procedure,
124 using OriginPro 9.1 software.

125 *2.4 Compression test*

126 Mechanical tests were performed using a mechanical testing machine (EZ-SX,
127 Shimadzu, Japan) equipped with a 500 N load cell, as described in a previous work
128 [35]. Test specimens were cylinder-shaped scaffolds with a 1.3 cm diameter and an
129 average height of around 1 cm. The crosshead speed was set at 1 $mm \cdot min^{-1}$, and the
130 load was applied until the specimen was compressed to around 80% of its original
131 height before break. Compression resistance of five dried samples for each composition
132 was evaluated at room temperature and the stress was calculated by dividing the
133 applied force with the initial scaffold surface area, whereas strain was calculated from
134 the displacement of the scaffolds in relation to the original thickness. Young's modulus
135 (E) was also calculated as the slope of the linear elastic regime (0-15%).

136 *2.5 Scanning electron microscopy (SEM)*

137 SEM (Hitachi TM3030 Tabletop, Germany) equipped with Energy Dispersive
138 Spectroscopy (EDS) was utilised to study the scaffold inner morphology. The samples
139 were cut into small squares, fixed on the aluminium stub using carbon tape. For pore
140 size evaluation SEM images were analysed by ImageJ software.

141 *2.6 Water uptake (WU) measurements*

142 WU was calculated gravimetrically according to ASTM D570-98 [36] under
143 physiological conditions. Three specimens of each composition were weighed (W_0) and
144 immersed in 6 mL of a phosphate buffered saline (PBS) solution at pH 7.0 in order to
145 determine the WU profile at 37°C in an incubator (INCU-Line, VWR). Then, the samples
146 were removed from the buffer solution at fixed times, wiped with a paper and reweighed
147 (W_t). WU was calculated using the following equation [37]:

148 $$\mathrm{WU}\ (\%)=\frac{W_t-W_0}{W_0}\times 100 \qquad \text{Eq.1}$$

149 A graph depicting WU against time was plotted in order to determine the equilibrium
150 swelling.

151 *2.7 Degradation test*

152 The degradation degree (DD) was calculated gravimetrically under physiological
153 conditions. Three specimens of each composition were weighed (W_I) and immersed in 6
154 mL of a PBS solution at pH 7.0 in order to determine the degradation at 37 °C in an
155 incubator. Samples were removed from the buffer solution once swelling test ended,
156 wiped with a paper, left to dry at room temperature for 24 h and reweighed (W_F). DD
157 was calculated using the following equation:

158 $$\mathrm{DD}\ (\%)=1-\frac{W_F}{W_I}\times 100 \qquad \text{Eq.2}$$

159 *2.8 THC release*

160 UV-Vis spectroscopy is one of the methods to determine the release and
161 concentration of bioactives in buffer solutions. Firstly, the wavelength of maximum
162 absorbance for THC in PBS was measured (λ_{max} 280 nm) and then, standard solutions
163 of THC were prepared over a concentration range (0.31250-0.00977 mg/mL) to
164 establish a calibration curve (y=0.0314 + 2.2012x, R^2=0.9985).

165 THC release was determined by immersion of a quarter of a scaffold in 6 mL of a PBS
166 solution (pH 7.0) at 37 °C in an incubator. At particular time intervals (1, 2, 4, 8, 24, 28
167 and 96 h), aliquots of buffer (3 mL) were withdrawn, replaced with fresh buffer and
168 analysed by UV–Vis spectroscopy (Lambda 2S Perkin Elmer) at 280 nm. All tests were
169 carried out in triplicate and the results were expressed as % of released THC with
170 respect to the THC incorporated in the scaffold by employing the calibration curve.

171 *2.9 Biological characterisation*

172 *2.9.1 Cell culture*

173 Chondrocytes cells were differentiated from Human Bone Marrow Stromal Cells (Y201)
174 and cultured according the protocol described by Genever et al.[38] at 37 °C, 5% CO_2,
175 in Chondrocyte Growth Medium ready-to-use (PromoCell, UK).

176 In order to perform biocompatibility assays, the scaffolds were prepared according the
177 same procedure explained in 2.2 section with few modifications. Once gelatin solution
178 was prepared, 1 mL was poured into each well of a 48 multiwell plate in order to get
179 smaller scaffolds, which were subsequently cut in samples of 8 mm diameter and an
180 average height of around 2.5 mm. Each sample was put into a membrane-based cell
181 culture insert (Millicell, membrane pore size of 0.8 µm, Merck, Millipore, Germany). This

182 insertion was carried out in a class 2 laminar flow hood and each insert was placed in a
183 well of a 24 multiwell plate. Afterwards, the plate was placed below the UV light for 30
184 min in order to keep it sterile. A suspension of $20x10^4$ cells in Growth medium was
185 seeded dropwise (in 500 μL) on the top surface of the scaffolds and incubated at 37 °C,
186 5% CO_2 for 30 min. Then, fresh medium was added up to1 mL volume.

187 *2.9.2 Cytocompatibility study*

188 The Presto Blue assay was exploited to test the metabolic activity of cells seeded on
189 the scaffolds after 1, 3, 7 and 14 days of culture. A LS-50B Luminescence Spectrometer
190 (Perkin Elmer, Waltham, MA) was used to measure the fluorescence (560 nm excitation
191 and 590 nm emission) after 5 h of incubation with a 10% aliquot of Presto Blue (Thermo
192 Scientific, USA). The obtained values were corrected subtracting the average
193 fluorescence of control wells. Results were expressed as mean ± standard deviation.

194 *2.9.3 Cell fixation and probe staining for confocal microscopy*

195 Three and seven days after seeding cells on the scaffolds, cells were fixed using 4%
196 paraformaldehyde (Sigma Life Science) for 15 min at room temperature. Cells were
197 washed three times using 0.1% DPBS/Tween 20 (Sigma Life Science), followed by a
198 20-min light-protected incubation period at room temperature with phalloidin (1 mg/mL,
199 Sigma Life Science). After three new washes with 0.1% DPBS/Tween 20, 4′,6-
200 diamidino-2-phenylindole (DAPI; 1:2500 solution, Vector Laboratories) was added, and
201 the solution was subjected to a 10-min light-protected incubation period at room
202 temperature. Afterwards, cells were washed and resuspended in 500 μL of 0.1%
203 DPBS/Tween 20. Fixed cells were protected from light and stored at 4 °C. Cells were

204 visualised using a Leica TCS SP2 UV AOBS MP (Upright) point scanning confocal
205 microscope (Leica Microsystems) at 20× magnification.

206 *2.10 Antibacterial tests*

207 Antimicrobial activity of the scaffolds was tested against *Staphylococcus aureus* (*S.*
208 *aureus*) NCTC 8325 and a clinical strain of *Pseudomonas aeruginosa* (*P. aeruginosa*)
209 (SOM-1, Stafford group culture collection). Fresh 4 h cultures of *S. aureus* strain 8325
210 and a clinical *P. aeruginosa* isolate (Sheffield culture collection) were grown in Brain
211 Heart Infusion broth (Oxoid) at 37°C (OD600 0.4-0.6) and spread onto Columbia
212 nutrient agar plates. After drying for 10 min, 8 mm HT gelatin scaffolds of both
213 concentration with or without THC were placed on the surface of the agar plates, which
214 were then incubated for 24 h at 37 °C before being photographed.

215 *2.11 Statistical analysis*

216 Data were subjected to one-way analysis of variant (ANOVA) by means of a SPSS
217 computer program (SPSS Statistic 20.0). Post hoc multiple comparisons were
218 determined by the Tukey's test with the level of significance set at $*p < 0.05$ and $**p <$
219 0.01.

220 **3. Results and discussion**

221 *3.1. Physicochemical characterisation*

222 ATR-FTIR analysis was carried out in order to evaluate the gelatin-lactose and
223 gelatin-THC interactions. The relative spectra are shown in **Figure 1A** and **1B**. The
224 main absorption bands were located in the spectral range from 1630 to 800 cm^{-1}.
225 Gelatin bands were related to C=O stretching at 1630 cm^{-1} (amide I), N-H bending at
226 1530 cm^{-1} (amide II) and C-N stretching at 1230 cm^{-1} (amide III) [39]. The main

227 absorption bands of glycerol were related to the five peaks corresponding to the
228 vibrations of C-C bonds at 850, 940 and 1000 cm^{-1} and C-O bonds at 1050 and 1100
229 cm^{-1} [40]. The bands associated with lactose were located between 1180 and 953 cm^{-1},
230 where the bands at 979 and 987 cm^{-1} were referred to the vibration of C-C, and the
231 band at 1034 cm^{-1} was associated with the vibration of C-O in CH_2-OH group [41].
232 Finally, the characteristic bands of THC corresponding to C=C stretching of aromatic
233 rings (1600-1400 cm^{-1}) and associated to C-O stretching of hydroxyl groups (1300-1000
234 cm^{-1}) cannot be clearly distinguished due the overlapping with the bands of gelatin and
235 glycerol [42].

236 As can be observed in **Figure 1A** and **1B**, the two bands situated in the range of
237 1100-1000 cm^{-1} tend to become a single band in HT scaffolds irrespective of gelatin
238 concentration, indicating the chemical reaction between gelatin and lactose, as shown
239 in previous works [32, 33]. As can be seen in **Scheme 1**, this cross-linking reaction is a
240 condensation reaction between the carbonyl group of lactose and the amino group of
241 gelatin, mainly the amino group of lysine [43, 44].

242 Regarding THC addition, the band corresponding to amide II showed a shoulder at
243 lower frequencies, attributed to the hydrogen bonding between the hydroxyl groups of
244 THC and the amino groups of proline and hydroxyproline in gelatin [45]. Additionally, the
245 bands in the range of 1100-1000 cm^{-1} were clearly distinguishable, indicating that THC
246 addition could hinder the chemical reaction between gelatin and lactose due to steric
247 hindrance. The band corresponding to amide I depends on the secondary structure of
248 the protein backbone and is the most commonly used band for the quantitative analysis
249 of conformational changes [46]. Therefore, the areas of the bands at 1624 cm^{-1}, 1650

250 cm^{-1}, and 1680 cm^{-1} as a function of protein concentration and heat treatment were
251 measured and shown in **Figure 1C**. As can be observed, the protein concentration did
252 not have great influence on NH scaffolds; however, it affected the secondary structure
253 of the protein in HT scaffolds. The increase of the bands at 1624 cm^{-1} and 1680 cm^{-1} in
254 HT scaffolds with 4% w/v gelatin could be related to a higher cross-linking degree in the
255 scaffolds with higher gelatin content. Regarding THC addition, the secondary structure
256 of the protein was affected to a lesser extent. This behaviour could be associated with a
257 lower cross-linking degree due to the fact that THC could hinder the cross-linking
258 reaction, irrespective of gelatin concentration.
259 Freeze-drying is a process in which a solvent is removed from a frozen product by a
260 sublimation process under vacuum, the removal of water could be influenced by the
261 initial gelatin concentration. As the dry product has smaller specific area at higher solute
262 concentrations, the removal of the absorbed water is more difficult (**Figure S1**),
263 requiring longer times to finish the secondary drying step [47]. Thus, the amount of
264 residual water present in gelatin scaffolds after freeze-drying could vary as a function of
265 the initial gelatin concentration, having a significant impact on the extension of cross-
266 linking reaction. In fact, moisture content is believed to be an important factor since
267 moisture can increase chains' mobility and, thus, the rate of chemical reaction [48].
268 *3.2. Mechanical and morphological characterisation*
269 In order to assess the effects of the initial gelatin concentration, THC addition and
270 cross-linking on mechanical properties of the scaffolds, the stress-strain curves,
271 obtained by compression tests at 0-80% strain, were analysed and the results are
272 shown in **Figure 2A**. All the samples presented the typical trend of porous scaffolds, in

273 which the stress-strain curve is comprised of three regions with different mechanical
274 behaviour: (i) the linear proportion of the stress-strain curve at low strain values is
275 related to the elastic behaviour of the material; (ii) the region at intermediate strain
276 values is related to the viscoelastic behaviour of the scaffold; and (iii) the curve at high
277 strain values is related to the densification process [49]. It is worth noting that increasing
278 the initial gelatin concentration and promoting the cross-linking reaction by heating
279 notably reinforced the scaffolds, indicating the relevance of these two factors[50]. As
280 can be seen in **Figure 2B**, the stress values at 40% strain for the gelatin scaffolds
281 without THC were significantly ($p < 0.05$) different. In fact, the strength enhancement
282 with respect to NH scaffolds with 2.5% w/v gelatin was 134% for HT scaffolds with 2.5%
283 w/v gelatin, 163% for NH scaffolds with 4% w/v gelatin, and 218% for HT scaffolds with
284 4% w/v gelatin. Regarding THC addition, a decrease in the scaffold reinforcement was
285 observed, which could be related to a lower cross-linking degree between gelatin and
286 lactose, as shown by ATR-FTIR. In fact, at 40% strain, the stress values of HT-THC
287 scaffolds with 2.5% w/v gelatin and 4% w/v gelatin were significantly ($p < 0.05$) lower
288 than those of HT scaffolds.

289 The Young's modulus of each scaffold was also calculated. Although 2.5% w/v
290 scaffolds did not show significant ($p > 0.05$) changes after both heat treatment and THC
291 addition, scaffolds prepared with 4% w/v gelatin presented a significant ($p < 0.05$)
292 increase after heat treatment. This could be due to a higher degree of cross-linking
293 between gelatin and lactose. However, the addition of THC slightly decreased the
294 modulus value due to its possible effect in slowing down the cross-linking reaction.

295 However, the obtained scaffolds presented suitable mechanical properties for cartilage
296 tissue engineering applications [51-53].

297 As freeze-drying is one of the most effective methods to create numerous cavities
298 within the bulk material, SEM analysis was performed on the fractured sections of the
299 scaffolds to evaluate the effect of the initial gelatin concentration, THC addition and the
300 heat treatment on the morphology and porosity of the scaffolds (**Figure 3**). It is worth
301 mentioning that the initial gelatin concentration notably affected the scaffolds porosity.
302 NH samples prepared with 2.5% w/v gelatin (**Figure 3A**) presented a homogeneous
303 porous matrix with small pores, which could provide more surface area for cell
304 adhesion. In contrast, a less porous structure with larger pores was shown when gelatin
305 concentration was increased up to 4% w/v (**Figure 3D**); this could facilitate nutrition
306 supply and waste removal [54]. The porosity and the pore size of the scaffolds
307 fabricated by freeze-drying are largely dependent on parameters such as the
308 water:polymer ratio and the viscosity of the solution [55]. In fact, when the initial gelatin
309 concentration increased, the volume fraction occupied by the material itself also
310 increased, affecting the porosity of the material [56]. Regarding heat treatment (**Figure**
311 **3B** and **E**), the reaction between gelatin and lactose led to more porous structures,
312 which presented lower pore size when THC was added (**Figure 3C** and **F**) mainly in 4%
313 w/v gelatin scaffolds.

314 As the distribution of the pore sizes is influenced by the composition, ImageJ
315 computer software was used to analyse SEM images and measure the pore sizes by
316 means of an estimation of the cross-sectional area of the scaffold [57]. **Figure 4A**
317 shows the average pore size of the scaffolds as a function of initial gelatin

318 concentration, THC addition and heat treatment. As can be observed, 2.5% w/v
319 scaffolds did not present notable changes in the average pore size while an increase in
320 pore size was observed when initial gelatin concentration increased. In fact, NH and HT
321 samples prepared with 4% w/v gelatin presented 2- and 3-fold average pore size with
322 larger pores (~ 197 μm and 170 μm) than NH and HT 2.5% w/v scaffolds (~ 86 μm and
323 65 μm), respectively. Regarding THC addition, samples prepared with 2.5% w/v gelatin
324 did not present significant ($p > 0.05$) changes while 4% w/v scaffolds pore size notable
325 decreased. This could be related to a higher volume occupied by the material in
326 samples prepared with 4% w/v gelatin.

327 The mean pore size distribution of the scaffolds as a function of initial gelatin
328 concentration, THC addition and heat treatment is shown in **Figure 4B**. In the case of
329 NH, HT and HT-THC scaffolds prepared with 2.5% w/v gelatin, around 74%, 66% and
330 62% of pores were in the size range of 50-100 μm, respectively. When gelatin
331 concentration was increased, it was observed a large number of pores in the size
332 ranges of 150-250 μm, 100-250 μm and 50-150 μm. These results indicated that gelatin
333 concentration, THC addition and heat treatment notable affected the pore size
334 distribution of scaffolds. Thus, NH and HT 4% w/v scaffolds showed bigger pore size,
335 which could explain lower deformation values [10], as shown by compression results.
336 Regarding THC addition, a decrease in pores size was observed which could be related
337 to a higher compaction of these scaffolds.

338 *3.3. Water uptake, degradation and THC release*

339 WU measurements were carried out in order to determine the effect of the initial
340 gelatin concentration, THC addition and the heat treatment on the water absorption

341 capacity of the scaffolds. As can be observed in **Figure S2**, NH scaffolds with 2.5% w/v
342 gelatin were completely dissolved after 30 min of immersion in PBS at 37 ºC and
343 considered not suitable, while HT and HT-THC scaffolds with 2.5% w/v gelatin
344 maintained their physical integrity, demonstrating the effect of heating to promote cross-
345 linking reaction [32]. Similar behaviour was observed for the scaffolds with 4% w/v
346 gelatin (data not shown).

347 WU capacities of HT and HT-THC scaffolds were analysed as a function of gelatin
348 concentration and the results are shown in **Figure 5.** As can be seen, gelatin
349 concentration notably affected the WU capacity. Although both HT scaffolds increased
350 their weight up to 400% after only 1 h of incubation in PBS, 4% w/v scaffolds (**Figure**
351 **5B**) took twice as long (48 h) to reach the same WU (~ 770%) as the 2.5% w/v scaffolds
352 (**Figure 5A**). However, WU results showed high absorption capacity (> 800%) for the
353 scaffolds prepared with both concentrations. These WU results showed that the
354 scaffolds were hydrophilic in nature with capacity to hold a large amount of water
355 molecules. However, the ability of the scaffold to hold water molecules within its network
356 is dependent on the architecture of the scaffolds [58]. The longer stability of HT
357 scaffolds with 4% w/v gelatin in PBS at 37 ºC could be related to a higher cross-linking
358 degree, lower porosity and higher compaction, which could slow down the absorption of
359 liquid, leading to longer times (> 336 h) than the scaffolds with 2.5% w/v (72 h) before
360 complete dissolution.

361 With regard to THC addition, an increase in the scaffold WU capacity was observed,
362 irrespective of gelatin concentration. In fact, WU values of the scaffolds with 4% w/v
363 gelatin increased up to 843 ± 20%, while the values of the scaffolds with 2.5% w/v

364 gelatin presented a higher capacity to retain water (946 ± 72%) after 48 h of incubation.
365 This faster WU for HT-THC scaffolds with 2.5% w/v gelatin can be due to the lower
366 cross-linking degree and compaction of these scaffolds. It is also worth noting that the
367 addition of THC facilitated the disintegration of scaffolds.

368 Scaffold degradation degree (DD) was calculated as well and the results are shown in
369 **Figure 5C**. With respect to NH scaffolds, DD values notably decreased up to 67.5 ±
370 0.2% and 12.1 ± 2.5% for the HT scaffolds with 2.5 and 4% w/v gelatin, respectively,
371 after 72 and 336 h of incubation in PBS at 37 ºC. This decrease was related to the
372 cross-linking reaction between gelatin and lactose. Since the degree of cross-linking
373 and compaction were higher for the scaffolds with 4% w/v gelatin, as shown by ATR-
374 FTIR and SEM results, these scaffolds showed lower DD values. Regarding THC
375 addition, the scaffolds with 2.5% w/v gelatin were totally degraded, while the scaffolds
376 with 4% w/v gelatin presented a degradation value of 54.6 ± 5.6% after 72 and 336 h of
377 incubation in PBS, respectively. As previously explained, the increase in the
378 degradation values of HT-THC scaffolds could be related to a lower extension of the
379 cross-linking reaction due to formation of physical bonds between the hydroxyl groups
380 of THC and the amino groups of proline and hydroxyproline in gelatin, which could
381 hinder the cross-linking reaction, resulting in higher DD values of HT-THC scaffolds
382 than those of HT scaffolds.

383 Finally, the THC release was analysed by UV-Vis spectroscopy and the results are
384 shown in **Figure 6**. As can be seen, in the first 8 h 82 ± 4% THC was released from
385 2.5% w/v scaffolds while 64 ± 9% was released from 4% w/v scaffolds. This decrease in
386 THC release could be due to a higher physical interaction between gelatin and THC, a

387 more extensive chemical reaction and a higher structural compaction in 4% w/v
388 scaffolds that slowed down the release of the bioactive. The high release of the anti-
389 inflammatory bioactive in the first 8 h could contribute to reduce the early postoperative
390 inflammation, improving the cartilage healing. Furthermore, the release of THC from
391 scaffolds continued increasing slightly over time since 2.5% w/v scaffolds presented a
392 complete THC release after 96 h of immersion due to scaffolds total degradation while
393 4% w/v scaffolds showed a lower THC release values (79 ± 9%). This controllable long
394 release of the anti-inflammatory compound could be an effective intra-articular drug
395 delivery method for the postoperative inflammation and pain management [59].

396 *3.4. Biological characterisation*

397 Due to the poor water stability of NH scaffolds, the biological characterisation was
398 only carried out for HT and HT-THC scaffolds as a function of gelatin concentration in
399 order to analyse the viability of those scaffolds as cell substrate materials. Cell
400 metabolic activity as well as cell morphology are shown in **Figure 7**. The metabolic
401 activity on both gelatin concentrations presented a similar behaviour being higher for the
402 2.5% w/v scaffolds without the presence of THC. The seeded chondrocytes presented
403 their metabolic activity peak on day 7, decreasing afterwards due to the high cell
404 confluence (as statistically significantly evident for the control represented by cells
405 seeded on Tissue Cultured Plate, TCP). It is important to note that the metabolic activity
406 on THC scaffolds was lower due to the THC presence; however, once released
407 (approximately 98 h as shown previously in section 3.3), cells achieved their maximum
408 metabolic activity. This is also related to the lower metabolic activity observed in the 4%

409 w/v scaffolds, since their THC release was slower when compared to the 2.5% w/v
410 scaffolds.

411 Phalloidin and Dapi stainings was performed to study the cell morphology and
412 organisation within the different scaffolds. As shown in **Figure 7**, the cells seeded in
413 both, 2.5 and 4% gelatin scaffolds, showed a high metabolic activity and spreading at
414 day 3; particularly with visualisation of typical polygon shape of young chondrocytes at
415 4% gelatin [60, 61]. Subsequently, as the cells proliferated, it was possible to observe
416 the formation of cellular clusters in the 4% w/v scaffolds, either in presence and
417 absence of THC, upon 7 days of culture. Furthermore, cultured cells were gradually
418 aggregating, retaining typical polygons shapes and creating large interspaces;
419 suggesting a potential formation of lacuna-like cartilage [62]. In contrast, the cells in the
420 TCP control and 2.5% gelatin groups showed lower expression of F-actin (phalloidin
421 staining). This could be induced by the different level of gelatin and/or its biomechanical
422 effects closer to natural cartilage tissues, by providing an environment with more
423 favourable chondrogenic properties [63]. It is also verified that both gelatin
424 concentrations, with or without THC, showed healthy and proliferating cells in the
425 developed scaffolds. Interestingly, the stability and metabolic activity of the scaffolds in
426 growth media improved up to 2 weeks when compared to TCP control group, and it
427 could be that the specific biological properties of gelatin to promote cell adhesion and
428 cell-maritx interactions enhanced the biological stability of scaffolds [64].

429 *3.5. Antibacterial characterisation*

430 In order to test the potential antimicrobial activity of THC infiltrated disks as an
431 additional feature of this material, we performed antimicrobial plate assays with disk-

432 shaped scaffolds (8 mm diameter) in the presence of the common nosocomial and joint-
433 replacement/ wound infecting organisms *S. aureus* and *P. aeruginosa*. As shown in
434 **Figure 8**, there was a slight antimicrobial action exhibited by the THC containing
435 scaffolds with *S. aureus* in the area where the disks were placed (i.e. with the THC
436 there was a less dense growth), seen by individual colonies being visible, whereas
437 without the THC the bacteria grew all the way up to the scaffold. The same did not apply
438 for *P. aeruginosa*. We therefore have preliminary evidence that these materials have
439 possible antimicrobial capability that could augment their potential for clinical use in
440 orthopaedic surgery, because *S. aureus* strains represent a significant proportion of all
441 pathogens causing infections associated with orthopaedic implants, and the binding of
442 *S. aureus* to host tissues and plasma proteins is of critical importance in the
443 development of infections at the implant site [65].

444 **4. Conclusions**

445 This study demonstrated the utility of lactose cross-linking and THC to modify and
446 improve the physico-chemical properties of gelatin-based porous scaffolds for tissue
447 engineering. The cross-linking reaction resulted in a more water stable scaffold with
448 enhanced mechanical properties and high water uptake capacity (> 800%). Although
449 porosity decreased with the increase of the initial gelatin concentration, the observed
450 increase of pore size from 118 ± 40 μm to 254 ± 57 μm, along with the cross-linking
451 reaction, reinforced the scaffolds, enhancing their mechanical properties. Results of *in*
452 *vitro* THC release and antibacterial experiments demonstrated that the THC-loaded
453 scaffolds were capable of effectively releasing THC in a controlled way, with 80% THC
454 released within three days that may lead to the design of an appropriate drug delivery

method for the postoperative inflammation and pain management. Looking forward to the intended clinical use, the main advantage of the system reported here was the THC biocompatibility and antimicrobial potential with ~~a~~ tailored concentrations for relatively rapid release to achieve a therapeutic effect minimising the risk of systemic side effects. This study has therefore demonstrated that THC may be applied to the manufacture of medical devices, particularly embedded in gelatin porous scaffolds, and it possesses potential antimicrobial properties to augment its' musculoskeletal applications.

Acknowledgments

Authors thank the University of the Basque Country (research group PPG17/18), the Provincial Council of Gipuzkoa (Department of Economic Development, the Rural Environment and Territorial Balance), the School of Engineering at Newcastle University (UK), and the EPSRC for their financial support. Also thanks both the National EPSRC XPS Users' Service (NEXUS) and Northern Institute for Cancer Research at Newcastle University. Alaitz Etxabide thanks UPV/EHU (DOCREC17/04).

469 **Figure captions**

470 **Figure 1** ATR-FTIR spectra of non-heated (NH), heat-treated (HT) and HT-THC
471 scaffolds with **(A)** 2.5 and **(B)** 4% w/v gelatin; **(C)** measurement of the areas of the
472 bands at 1624 cm^{-1}, 1650 cm^{-1}, and 1680 cm^{-1} as a function of protein concentration
473 and heat treatment.

474 **Figure 2 (A)** Stress-strain curves of non-heated (NH), heat-treated (HT) and HT-THC
475 scaffolds with 2.5 and 4% w/v gelatin. **(B)** Young's modulus and stress values
476 (calculated at 40% strain). Two means followed by the same letter in the same
477 parameter are not significantly ($p > 0.05$) different through the Tukey's multiple range
478 test. n = 3 is the minimum number of replications.

479 **Figure 3** SEM micrographs of **(A)** non-heated (NH), **(B)** heat-treated (HT) and **(C)** HT-
480 THC scaffolds with 2.5% w/v gelatin and **(D)** NH, **(E)** HT and **(F)** HT-THC scaffolds with
481 4% w/v gelatin. Bar = 200 µm.

482 **Figure 4 (A)** Average pore size (µm) and **(B)** pore size distribution (%) of non-heated
483 (NH) heat-treated (HT) and HT-THC scaffolds with 2.5 and 4% w/v gelatin.

484 **Figure 5** Water uptake (WU) values for heat-treated (HT) and HT-THC scaffolds with
485 **(A)** 2.5 and **(B)** 4% w/v gelatin. **(C)** Scaffold degradation degree (DD) values calculated
486 after immersion in PBS for different interval times. Two means followed by the same
487 letter are not significantly ($p > 0.05$) different through the Tukey's multiple range test. n
488 = 3 is the minimum number of replications.

489 **Figure 6** THC release from heat-treated (HT) scaffolds with 2.5 and 4% w/v gelatin.

490 **Figure 7** Metabolic activity and morphological study of cells seeded on the porous
491 scaffolds. PrestoBlue assay of cells cultured on **(A)** 2.5% w/v and **(B)** 4% w/v gelatin
492 porous scaffolds after 1, 3, 7 and 14 days. **(C)** Confocal microscopy images of
493 chondrocytes cells after 3 and 7 days of culture. Scale bars: 75 µm.

494 **Figure 8** Representative macro-photograph showing growth inhibition of (**A**)
495 *Pseudomonas aeuroginosa* and (**B**) *Staphylococcus aureus* at 24 h by 2.5% w/v gelatin
496 without and with THC addition (a and c), and 4% w/w gelatin without and with THC
497 addition (b and d).

498 **Scheme 1**. The early stage of the cross-linking reaction (gal=galactose).

499

500 A. Etxabide, R.D.C. Ribeiro, P. Guerrero, A.M. Ferreira, G.P. Stafford, K. Dalgarno, K.
501 de la Caba, P. Gentile. *International Journal of Biological Macromolecules*

502 **Figure 1**

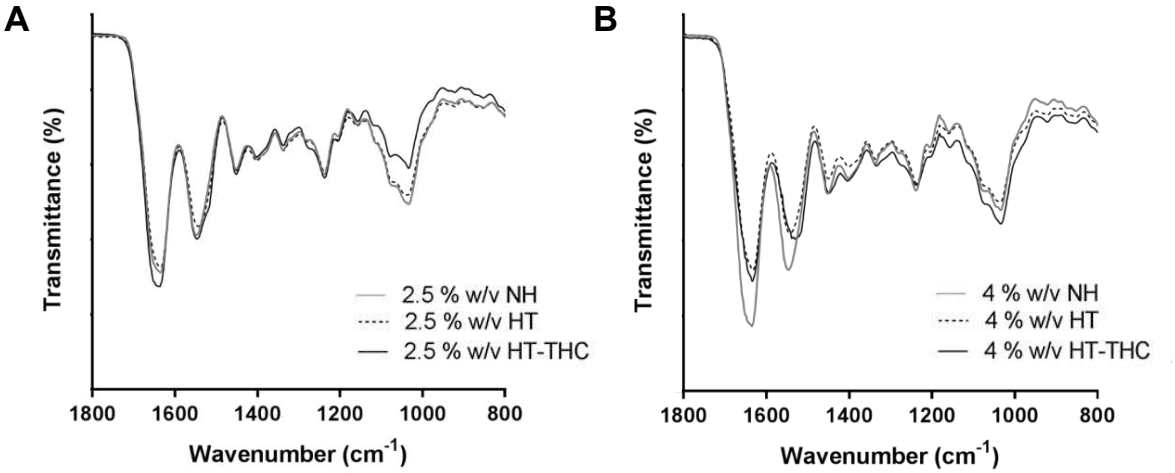

C

Gelatin concentration	Scaffold	1624 cm^{-1}	1650 cm^{-1}	1680 cm^{-1}
2.5% w/v	NH	35.7	60.1	4.2
	HT	42.1	52.3	5.6
	HT-THC	40.9	54.4	4.7
4.0% w/v	NH	35.5	59.4	5.1
	HT	48.2	44.3	7.5
	HT-THC	46.9	46.3	6.8

503
504

Figure 2

A

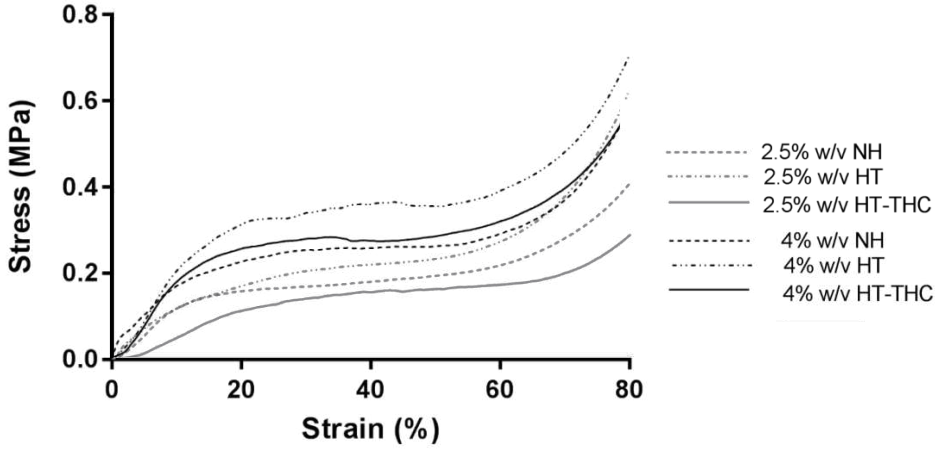

B

Scaffold	Stress (MPa)		Young's modulus (MPa)	
	2.5% w/v	**4.0% w/v**	**2.5% w/v**	**4.0% w/v**
NH	0.173 ± 0.006[a]	0.282 ± 0.04[c]	1.22 ± 0.18[a]	1.51 ± 0.04[ab]
HT	0.232 ± 0.011[bc]	0.377 ± 0.050[d]	1.42 ± 0.18[ab]	2.43 ± 0.48[c]
HT-THC	0.155 ± 0.003[a]	0.289 ± 0.014[c]	0.92 ± 0.22[a]	2.04 ± 0.18[bc]

A. Etxabide, R.D.C. Ribeiro, P. Guerrero, A.M. Ferreira, G.P. Stafford, K. Dalgarno, K. de la Caba, P. Gentile. *International Journal of Biological Macromolecules*

Figure 3

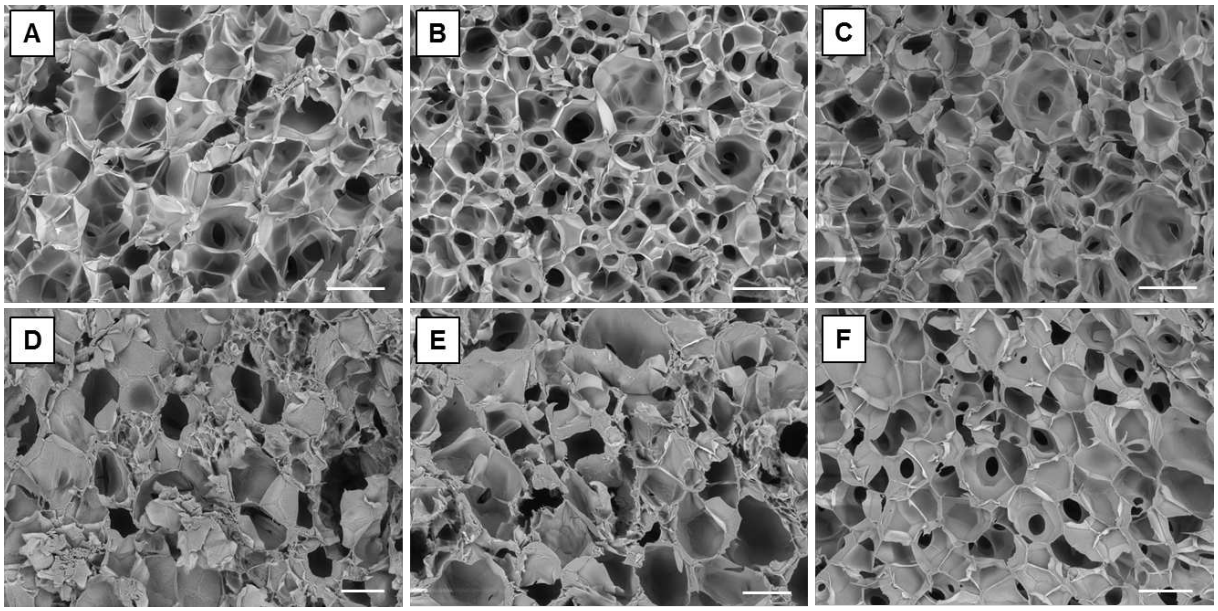

516 A. Etxabide, R.D.C. Ribeiro, P. Guerrero, A.M. Ferreira, G.P. Stafford, K. Dalgarno, K.
517 de la Caba, P. Gentile. *International Journal of Biological Macromolecules*
518 **Figure 4**

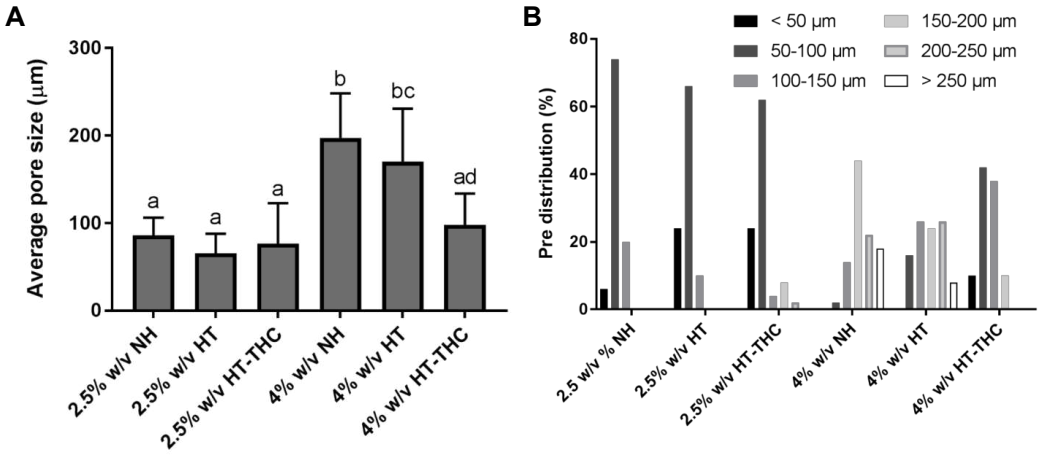

519
520

521 A. Etxabide, R.D.C. Ribeiro, P. Guerrero, A.M. Ferreira, G.P. Stafford, K. Dalgarno, K.
522 de la Caba, P. Gentile. *International Journal of Biological Macromolecules*
523 **Figure 5**

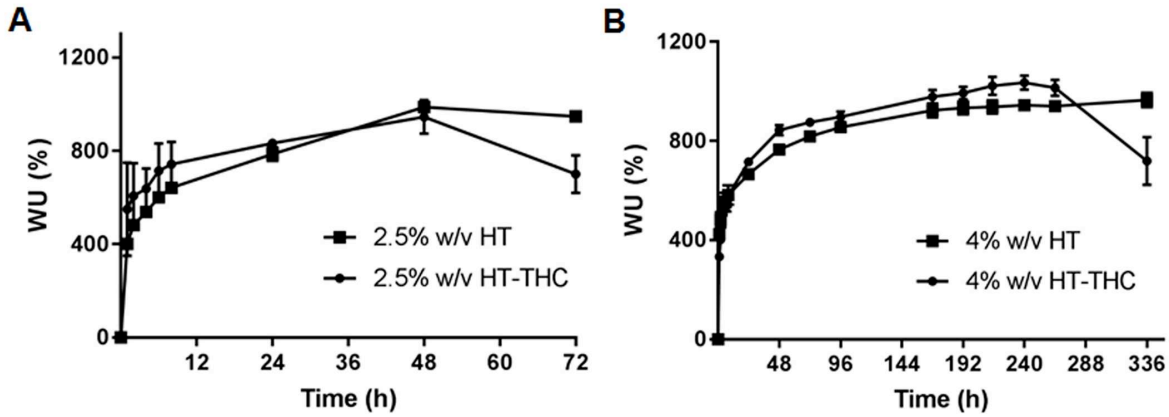

C

Scaffold	2.5% w/v		4.0% w/v	
	t (h)	DD (%)	t (h)	DD (%)
NH	0.5	100.0 ± 0.0[a]	0.5	100.0 ± 0.0[a]
HT	72	67.5 ± 12.6[b]	336	12.1± 2.5[c]
HT-THC	72	100.0 ± 0.0[a]	336	54.5 ± 5.6[b]

524
525

526 A. Etxabide, R.D.C. Ribeiro, P. Guerrero, A.M. Ferreira, G.P. Stafford, K. Dalgarno, K.
527 de la Caba, P. Gentile. *International Journal of Biological Macromolecules*
528 **Figure 6**

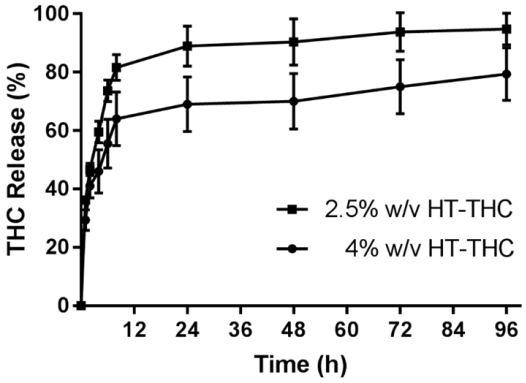

529
530

A. Etxabide, R.D.C. Ribeiro, P. Guerrero, A.M. Ferreira, G.P. Stafford, K. Dalgarno, K. de la Caba, P. Gentile. *International Journal of Biological Macromolecules*

Figure 7

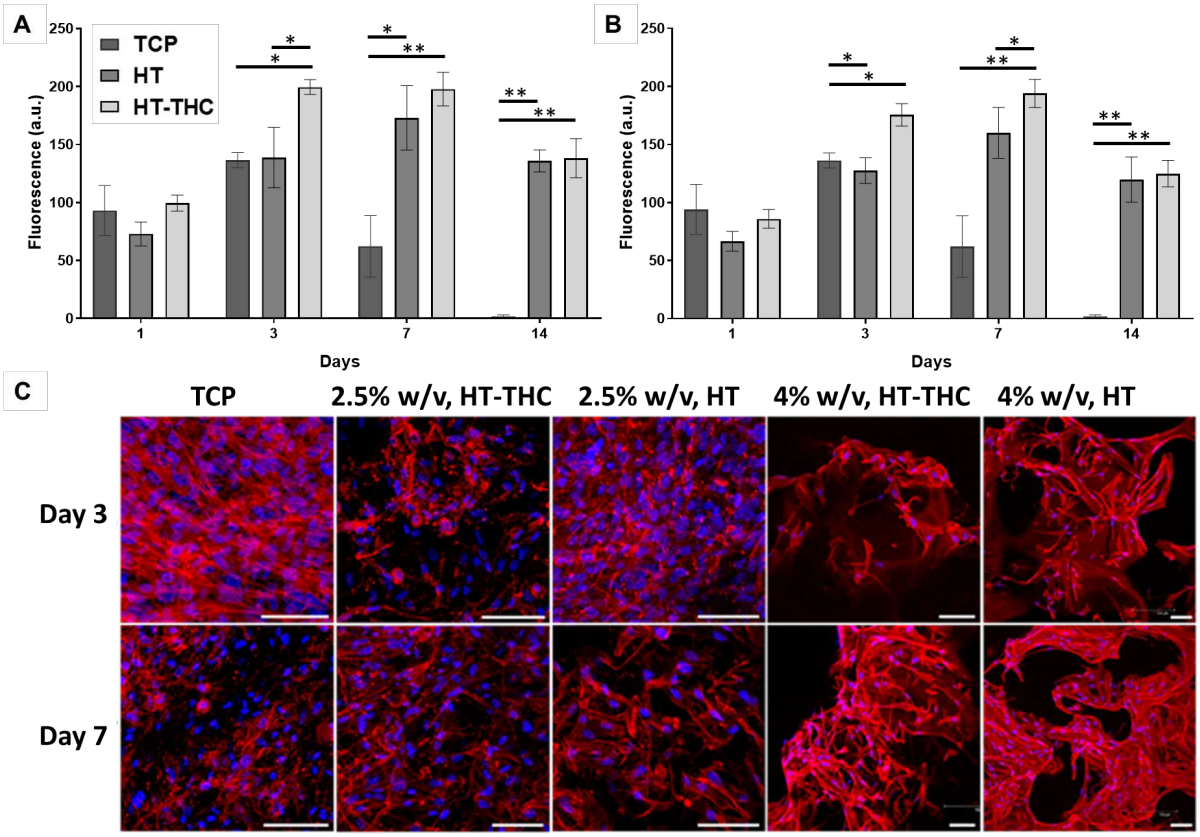

A. Etxabide, R.D.C. Ribeiro, P. Guerrero, A.M. Ferreira, G.P. Stafford, K. Dalgarno, K. de la Caba, P. Gentile. *International Journal of Biological Macromolecules*

Figure 8

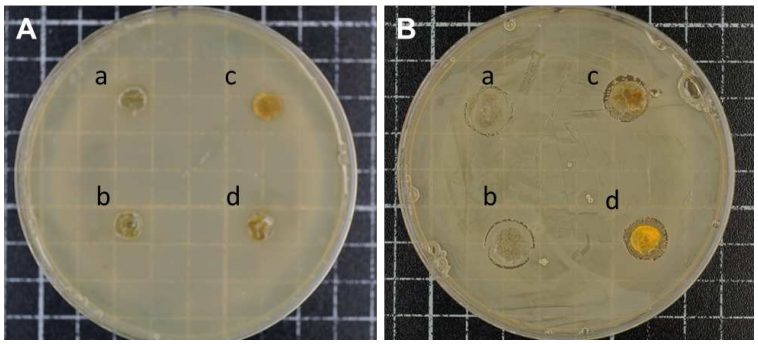

A. Etxabide, R.D.C. Ribeiro, P. Guerrero, A.M. Ferreira, G.P. Stafford, K. Dalgarno, K. de la Caba, P. Gentile. *International Journal of Biological Macromolecules*

Scheme 1

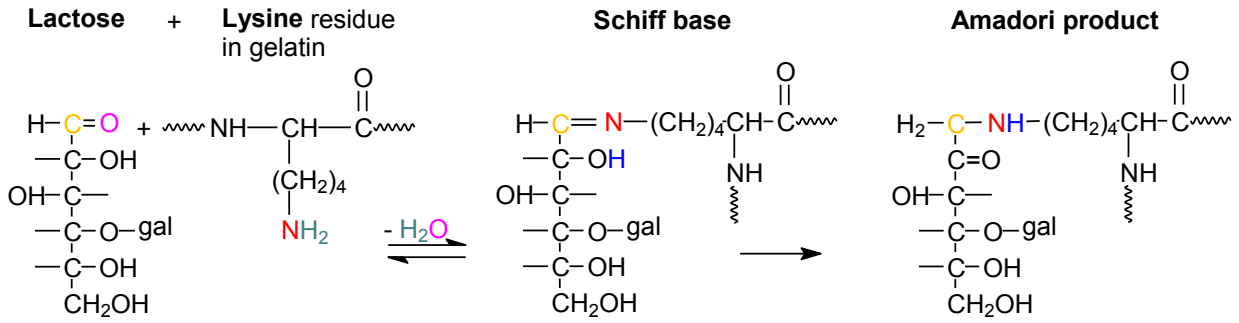

References

[1] Q. Zhang, H. Lu, N. Kawazoe, G. Chen, Pore size effect of collagen scaffolds on cartilage regeneration, Acta biomaterialia 10(5) (2014) 2005-2013.

[2] S.J. Hollister, Porous scaffold design for tissue engineering, Nature materials 4(7) (2005) 518-524.

[3] H. Lu, N. Kawazoe, T. Kitajima, Y. Myoken, M. Tomita, A. Umezawa, G. Chen, Y. Ito, Spatial immobilization of bone morphogenetic protein-4 in a collagen-PLGA hybrid scaffold for enhanced osteoinductivity, Biomaterials 33(26) (2012) 6140-6146.

[4] M.C. Echave, P. Sánchez, J.L. Pedraz, G. Orive, Progress of gelatin-based 3D approaches for bone regeneration, Journal of Drug Delivery Science and Technology (2017).

[5] A.I. Raafat, Gelatin based pH-sensitive hydrogels for colon-specific oral drug delivery: Synthesis, characterization, and in vitro release study, Journal of applied polymer science 118(5) (2010) 2642-2649.

[6] N.M. Siqueira, B. Paiva, M. Camassola, E.Q. Rosenthal-Kim, K.C. Garcia, F.P. dos Santos, R.M.D. Soares, Gelatin and galactomannan-based scaffolds: Characterization and potential for tissue engineering applications, Carbohydrate polymers 133 (2015) 8-18.

[7] T. Agarwal, R. Narayan, S. Maji, S. Behera, S. Kulanthaivel, T.K. Maiti, I. Banerjee, K. Pal, S. Giri, Gelatin/Carboxymethyl chitosan based scaffolds for dermal tissue engineering applications, International journal of biological macromolecules 93 (2016) 1499-1506.

[8] S. Kuttappan, D. Mathew, M.B. Nair, Biomimetic composite scaffolds containing bioceramics and collagen/gelatin for bone tissue engineering-A mini review, International journal of biological macromolecules 93 (2016) 1390-1401.

[9] A.A. Aldana, G.A. Abraham, Current advances in electrospun gelatin-based scaffolds for tissue engineering applications, International journal of pharmaceutics 523(2) (2017) 441-453.

[10] K.G. Shankar, N. Gostynska, M. Montesi, S. Panseri, S. Sprio, E. Kon, M. Marcacci, A. Tampieri, M. Sandri, Investigation of different cross-linking approaches on 3D gelatin scaffolds for tissue engineering application: A comparative analysis, International journal of biological macromolecules 95 (2017) 1199-1209.

[11] S. Chen, Q. Zhang, T. Nakamoto, N. Kawazoe, G. Chen, Gelatin scaffolds with controlled pore structure and mechanical property for cartilage tissue engineering, Tissue Engineering Part C: Methods 22(3) (2016) 189-198.

[12] C. Chung, J.A. Burdick, Engineering cartilage tissue, Advanced drug delivery reviews 60(2) (2008) 243-262.

[13] C. Tang, C. Jin, X. Du, C. Yan, B.-H. Min, Y. Xu, L. Wang, An Autologous Bone Marrow Mesenchymal Stem Cell–Derived Extracellular Matrix Scaffold Applied with Bone Marrow Stimulation for Cartilage Repair, Tissue Engineering Part A 20(17-18) (2014) 2455-2462.

[14] B.P. Chan, K.W. Leong, Scaffolding in tissue engineering: general approaches and tissue-specific considerations, European spine journal 17(4) (2008) 467-479.

[15] M. Nikkhah, M. Akbari, A. Paul, A. Memic, A. Dolatshahi-Pirouz, A. Khademhosseini, Gelatin-Based Biomaterials For Tissue Engineering And Stem Cell Bioengineering, Biomaterials from Nature for Advanced Devices and Therapies (2016) 37-62.

[16] P. Hernández-Muñoz, R. Villalobos, A. Chiralt, Effect of cross-linking using aldehydes on properties of glutenin-rich films, Food Hydrocolloids 18(3) (2004) 403-411.

[17] M. Lacroix, K.D. Vu, Edible coating and film materials: proteins, Innovations in Food Packaging (Second Edition), Elsevier2014, pp. 277-304.

[18] A. Ghosh, M.A. Ali, G.J. Dias, Effect of cross-linking on microstructure and physical performance of casein protein, Biomacromolecules 10(7) (2009) 1681-1688.

[19] J. Liu, Q. Ru, Y. Ding, Glycation a promising method for food protein modification: physicochemical properties and structure, a review, Food Research International 49(1) (2012) 170-183.

[20] G.B. Naranjo, A.S.P. Gonzales, G.E. Leiva, L.S. Malec, The kinetics of Maillard reaction in lactose-hydrolysed milk powder and related systems containing carbohydrate mixtures, Food chemistry 141(4) (2013) 3790-3795.
[21] A. Gaowa, T. Horibe, M. Kohno, K. Sato, H. Harada, M. Hiraoka, Y. Tabata, K. Kawakami, Combination of hybrid peptide with biodegradable gelatin hydrogel for controlled release and enhancement of anti-tumor activity in vivo, Journal of Controlled Release 176 (2014) 1-7.
[22] A.H. Nguyen, J. McKinney, T. Miller, T. Bongiorno, T.C. McDevitt, Gelatin methacrylate microspheres for controlled growth factor release, Acta biomaterialia 13 (2015) 101-110.
[23] A. Berardi, L. Bisharat, M. Cespi, I.A. Basheti, G. Bonacucina, L. Pavoni, H.S. AlKhatib, Controlled release properties of zein powder filled into hard gelatin capsules, Powder Technology 320 (2017) 703-713.
[24] S. Patel, S. Srivastava, M.R. Singh, D. Singh, Preparation and optimization of chitosan-gelatin films for sustained delivery of lupeol for wound healing, International journal of biological macromolecules (2017).
[25] P.H. Long, Medical devices in orthopedic applications, Toxicologic pathology 36(1) (2008) 85-91.
[26] M. Zilberman, J.J. Elsner, Antibiotic-eluting medical devices for various applications, Journal of Controlled Release 130(3) (2008) 202-215.
[27] A. Etxabide, V. Coma, P. Guerrero, C. Gardrat, K. De La Caba, Effect of cross-linking in surface properties and antioxidant activity of gelatin films incorporated with a curcumin derivative, Food hydrocolloids 66 (2017) 168-175.
[28] A. Etxabide, J. Uranga, P. Guerrero, K. de la Caba, Development of active gelatin films by means of valorisation of food processing waste: A review, Food Hydrocolloids 68 (2017) 192-198.
[29] M. Dai, X. Zheng, X. Xu, X. Kong, X. Li, G. Guo, F. Luo, X. Zhao, Y.Q. Wei, Z. Qian, Chitosan-alginate sponge: preparation and application in curcumin delivery for dermal wound healing in rat, BioMed Research International 2009 (2009).
[30] A.B. Hegge, T. Andersen, J.E. Melvik, E. Bruzell, S. Kristensen, H.H. Tønnesen, Formulation and bacterial phototoxicity of curcumin loaded alginate foams for wound treatment applications: studies on curcumin and curcuminoides XLII, Journal of pharmaceutical sciences 100(1) (2011) 174-185.
[31] C.N. Gajendragadkar, P.R. Gogate, Intensified recovery of valuable products from whey by use of ultrasound in processing steps–A review, Ultrasonics sonochemistry 32 (2016) 102-118.
[32] A. Etxabide, J. Uranga, P. Guerrero, K. de la Caba, Improvement of barrier properties of fish gelatin films promoted by gelatin glycation with lactose at high temperatures, LWT-Food Science and Technology 63(1) (2015) 315-321.
[33] A. Etxabide, M. Urdanpilleta, P. Guerrero, K. de la Caba, Effects of cross-linking in nanostructure and physicochemical properties of fish gelatins for bio-applications, Reactive and Functional Polymers 94 (2015) 55-62.
[34] A. Etxabide, C. Vairo, E. Santos-Vizcaino, P. Guerrero, J.L. Pedraz, M. Igartua, K. de la Caba, R.M. Hernandez, Ultra thin hydro-films based on lactose-crosslinked fish gelatin for wound healing applications, International journal of pharmaceutics 530(1-2) (2017) 455-467.
[35] B.P. Kanungo, E. Silva, K. Van Vliet, L.J. Gibson, Characterization of mineralized collagen–glycosaminoglycan scaffolds for bone regeneration, Acta Biomaterialia 4(3) (2008) 490-503.
[36] D. ASTM, 570-98, Standard test method for water absorption of plastics (2005).
[37] A. Martínez-Ruvalcaba, F. Becerra-Bracamontes, J.C. Sánchez-Díaz, A. González-Álvarez, Polyacrylamide-gelatin polymeric networks: effect of pH and gelatin concentration on the swelling kinetics and mechanical properties, Polymer bulletin 62(4) (2009) 539-548.
[38] S. James, J. Fox, F. Afsari, J. Lee, S. Clough, C. Knight, J. Ashmore, P. Ashton, O. Preham, M. Hoogduijn, Multiparameter analysis of human bone marrow stromal cells identifies distinct immunomodulatory and differentiation-competent subtypes, Stem Cell Reports 4(6) (2015) 1004-1015.

[39] N. BenBettaïeb, T. Karbowiak, S. Bornaz, F. Debeaufort, Spectroscopic analyses of the influence of electron beam irradiation doses on mechanical, transport properties and microstructure of chitosan-fish gelatin blend films, Food Hydrocolloids 46 (2015) 37-51.
[40] S. Basu, U.S. Shivhare, T.V. Singh, V.S. Beniwal, Rheological, textural and spectral characteristics of sorbitol substituted mango jam, Journal of Food Engineering 105(3) (2011) 503-512.
[41] W.-q. Wang, Y.-h. Bao, Y. Chen, Characteristics and antioxidant activity of water-soluble Maillard reaction products from interactions in a whey protein isolate and sugars system, Food chemistry 139(1) (2013) 355-361.
[42] H. Souguir, F. Salaün, P. Douillet, I. Vroman, S. Chatterjee, Nanoencapsulation of curcumin in polyurethane and polyurea shells by an emulsion diffusion method, Chemical engineering journal 221 (2013) 133-145.
[43] K. Siimon, H. Siimon, M. Järvekülg, Mechanical characterization of electrospun gelatin scaffolds cross-linked by glucose, Journal of Materials Science: Materials in Medicine 26(1) (2015) 37.
[44] A. Bigi, G. Cojazzi, S. Panzavolta, N. Roveri, K. Rubini, Stabilization of gelatin films by crosslinking with genipin, Biomaterials 23(24) (2002) 4827-4832.
[45] K.M. Rao, K.S.V.K. Rao, G. Ramanjaneyulu, C.-S. Ha, Curcumin encapsulated pH sensitive gelatin based interpenetrating polymeric network nanogels for anti cancer drug delivery, International journal of pharmaceutics 478(2) (2015) 788-795.
[46] N. Dave, A. Troullier, I. Mus-Veteau, M. Duñach, G. Leblanc, E. Padrós, Secondary structure components and properties of the melibiose permease from Escherichia coli: a Fourier transform infrared spectroscopy analysis, Biophysical Journal 79(2) (2000) 747-755.
[47] X.C. Tang, M.J. Pikal, Design of freeze-drying processes for pharmaceuticals: practical advice, Pharmaceutical research 21(2) (2004) 191-200.
[48] C.W. Wong, H.B. Wijayanti, B.R. Bhandari, Maillard reaction in limited moisture and low water activity environment, Water Stress in Biological, Chemical, Pharmaceutical and Food Systems, Springer2015, pp. 41-63.
[49] C. Tonda-Turo, P. Gentile, S. Saracino, V. Chiono, V.K. Nandagiri, G. Muzio, R.A. Canuto, G. Ciardelli, Comparative analysis of gelatin scaffolds crosslinked by genipin and silane coupling agent, International journal of biological macromolecules 49(4) (2011) 700-706.
[50] J.-Y. Lai, D.H.-K. Ma, M.-H. Lai, Y.-T. Li, R.-J. Chang, L.-M. Chen, Characterization of cross-linked porous gelatin carriers and their interaction with corneal endothelium: biopolymer concentration effect, PLoS One 8(1) (2013) e54058.
[51] W. Chen, B. Sun, T. Zhu, Q. Gao, Y. Morsi, H. El-Hamshary, M. El-Newehy, X. Mo, Groove fibers based porous scaffold for cartilage tissue engineering application, Materials Letters 192 (2017) 44-47.
[52] R. Levato, W.R. Webb, I.A. Otto, A. Mensinga, Y. Zhang, M. van Rijen, R. van Weeren, I.M. Khan, J. Malda, The bio in the ink: cartilage regeneration with bioprintable hydrogels and articular cartilage-derived progenitor cells, Acta biomaterialia 61 (2017) 41-53.
[53] S. Wu, H. Dong, Q. Li, G. Wang, X. Cao, High strength, biocompatible hydrogels with designable shapes and special hollow-formed character using chitosan and gelatin, Carbohydrate Polymers 168 (2017) 147-152.
[54] M. Jafari, Z. Paknejad, M.R. Rad, S.R. Motamedian, M.J. Eghbal, N. Nadjmi, A. Khojasteh, Polymeric scaffolds in tissue engineering: a literature review, Journal of Biomedical Materials Research Part B: Applied Biomaterials 105(2) (2017) 431-459.
[55] A.G. Mikos, J.S. Temenoff, Formation of highly porous biodegradable scaffolds for tissue engineering, Electronic Journal of Biotechnology 3(2) (2000) 23-24.
[56] X. Wu, Y. Liu, X. Li, P. Wen, Y. Zhang, Y. Long, X. Wang, Y. Guo, F. Xing, J. Gao, Preparation of aligned porous gelatin scaffolds by unidirectional freeze-drying method, Acta biomaterialia 6(3) (2010) 1167-1177.
[57] S.T. Ho, D.W. Hutmacher, A comparison of micro CT with other techniques used in the characterization of scaffolds, Biomaterials 27(8) (2006) 1362-1376.

[58] L.P. Yan, Y.J. Wang, L. Ren, G. Wu, S.G. Caridade, J.B. Fan, L.Y. Wang, P.H. Ji, J.M. Oliveira, J.T. Oliveira, Genipin-cross-linked collagen/chitosan biomimetic scaffolds for articular cartilage tissue engineering applications, Journal of Biomedical Materials Research Part A 95(2) (2010) 465-475.
[59] W.N. Scott, Insall & Scott Surgery of the Knee E-Book, Elsevier Health Sciences2011.
[60] J. Liu, X. Liu, G. Zhou, R. Xiao, Y. Cao, Conditioned medium from chondrocyte/scaffold constructs induced chondrogenic differentiation of bone marrow stromal cells, The Anatomical Record 295(7) (2012) 1109-1116.
[61] X. Li, X. Ren, S. Li, J. Liang, X. Zhao, T. Wang, Z. Wang, Morphological, Immunocytochemical, and Biochemical Studies of Rat Costal Chondrocytes Exposed to IL-1β and TGF-β1, Journal of healthcare engineering 2017 (2017).
[62] K. Yang, J. Sun, D. Wei, L. Yuan, J. Yang, L. Guo, H. Fan, X. Zhang, Photo-crosslinked mono-component type II collagen hydrogel as a matrix to induce chondrogenic differentiation of bone marrow mesenchymal stem cells, Journal of Materials Chemistry B 5(44) (2017) 8707-8718.
[63] K. Brodkin, A. Garcıa, M. Levenston, Chondrocyte phenotypes on different extracellular matrix monolayers, Biomaterials 25(28) (2004) 5929-5938.
[64] M. Santoro, A.M. Tatara, A.G. Mikos, Gelatin carriers for drug and cell delivery in tissue engineering, Journal of controlled release 190 (2014) 210-218.
[65] M.C. Hudson, W.K. Ramp, K.P. Frankenburg, Staphylococcus aureus adhesion to bone matrix and bone-associated biomaterials, FEMS microbiology letters 173(2) (1999) 279-284.